HHS Public Access

Author manuscript

Exp Mol Pathol. Author manuscript; available in PMC 2017 February 01.

Published in final edited form as:

Exp Mol Pathol. 2016 February ; 100(1): 92–100. doi:10.1016/j.yexmp.2015.11.018.

Genetic determinants of fibro-osseous lesions in aged inbred mice

Annerose Berndt[a], **Cheryl Ackert-Bicknell**[b,1], **Kathleen A. Silva**[b], **Victoria E. Kennedy**[b], **Beth A. Sundberg**[b], **Justin M. Cates**[c], **Paul N. Schofield**[b,d], and **John P. Sundberg**[b,*]

Annerose Berndt: berndta@upmc.edu; Cheryl Ackert-Bicknell: Cheryl_AckertBicknell@URMC.Rochester.edu; Kathleen A. Silva: kathleen.silva@jax.org; Victoria E. Kennedy: vicki.kennedy@jax.org; Beth A. Sundberg: beth.sundberg@jax.org; Justin M. Cates: justin.m.cates@Vanderbilt.Edu; Paul N. Schofield: PNS12@cam.ac.uk; John P. Sundberg: john.sundberg@jax.org

[a]Department of Medicine, University of Pittsburgh, Pittsburgh, PA, United States

[b]The Jackson Laboratory, Bar Harbor, ME, United States

[c]Department of Pathology, Microbiology and Immunology, Vanderbilt University School of Medicine, Nashville, TN, United States

[d]Department of Physiology, Development and Neuroscience, University of Cambridge, Cambridge, United Kingdom

Abstract

Fibro-osseous lesions in mice are progressive aging changes in which the bone marrow is replaced to various degrees by fibrovascular stroma and bony trabeculae in a wide variety of bones. The frequency and severity varied greatly among 28 different inbred mouse stains, predominantly affecting females, ranging from 0% for 10 strains to 100% for KK/HlJ and NZW/LacJ female mice. Few lesions were observed in male mice and for 23 of the strains, no lesions were observed in males for any of the cohorts. There were no significant correlations between strain-specific severities of fibro-osseous lesions and ovarian (r=0.11; P=0.57) or endometrial (r=0.03; P=0.89) cyst formation frequency or abnormalities in parathyroid glands. Frequency of fibro-osseous lesions was most strongly associated ($P < 10^{-6}$) with genome variations on chromosome (Chr) 8 at 90.6 and 90.8 Mb (rs33108071, rs33500669; $P = 5.0 \cdot 10^{-10}$, $1.3 \cdot 10^{-6}$), Chr 15 at 23.6 and 23.8 Mb (rs32087871, rs45770368; $P = 7.3 \cdot 10^{-7}$, $2.7 \cdot 10^{-6}$), and Chr 19 at 33.2, 33.4, and 33.6 Mb (rs311004232, rs30524929, rs30448815; $P=2.8 \cdot 10^{-6}$, $2.8 \cdot 10^{-6}$, $2.8 \cdot 10^{-6}$) in genome-wide association studies (GWAS). The relatively large number of candidate genes identified in the GWAS analyses suggests that this may be an extremely complex polygenic disease. These results indicate that fibro-osseous lesions are surprisingly common in many inbred strains of laboratory mice as they age. While this presents little problem in most studies that utilize young animals, it may complicate aging studies, particularly those focused on bone.

*Corresponding author at: The Jackson Laboratory, 600 Main Street, Bar Harbor, ME 04609-1500, United States.

[1]Current address: Center for Musculoskeletal Research, University of Rochester Medical Center, Rochester, NY, United States.

Disclosure

The authors state that they have no conflicts of interest.

Keywords

Bone; Genome-wide association studies; Aging; KK/HlJ mice

1. Introduction

Idiopathic bone lesions are rare in inbred mice. Apart from inherited bone abnormalities (Elefteriou and Yang 2011; Woodward and Montgomery 1978), “cage kyphosis” (Sass et al., 1976; Sokoloff and Habermann 1958), and bone and cartilage tumors (Kavirayani and Foreman 2010; Kavirayani et al., 2012), fibro-osseous lesions of the bone develop primarily in the sternebrae, long bones, and vertebrae of female mice. Most commonly, those changes have been reported for B6C3F1 mice (i.e., F1 hybrid mice generated by crossing C57BL/6 females with C3H/HeJ male mice) (Gervais and Attia 2005; Sass and Montali 1980). Lesions can be observed in mice as young as 32 weeks (i.e., 4.5 months) of age. At 110 weeks (i.e., 16 months) of age the frequency of the lesions is 100% in female and less than 1% in male B6C3F1 hybrid mice (Albassamet al., 1991; Sass and Montali 1980). Although the histologic features of fibro-osseous lesions have been described in detail, the strains affected, the underlying genetic predisposition, and pathogenesis of the disease are still unclear.

The comparison between fibro-osseous lesions in mice and humans is difficult. Fibro-osseous lesions in mice are morphologically similar to fibrous osteodystrophy and myelofibrosis in humans and other species. However, osteodystrophy is associated with renal or parathyroid pathophysiology and mice with fibro-osseous lesions show no evidence of renal or parathyroid dysfunction. Also, mice with fibro-osseous lesions do not have associated myeloproliferation, a common observation with myelofibrosis. Thus, it has been suggested that fibro-osseous lesions observed in aging mice have a distinct pathogenesis. There is evidence for an associated hormonal imbalance, based on a strong sexual dichotomy where females are almost exclusively affected. Also, when mice of both sexes are treated with estrogen, they developmore severe fibro-osseous lesions earlier than seen in the spontaneous disease (Highman et al., 1981; Sass and Montali 1980; Silberberg and Silberberg 1970). Fibro-osseous lesions in B6C3F1 mice are often accompanied by ovarian cysts and cystic endometrial hyperplasia and, thus, could be caused by estrogen-producing cysts (Sass and Montali 1980). Misoprostol, an analog of prostaglandin E1, produces bone changes similar to those caused by estrogens in mice (Dodd and Port 1987). Lesions were also associated with increased plasma alkaline phosphatase levels in aged B6C3F1 hybrid female mice (Albassam et al. 1991).

The most common fibro-osseous lesions seen in human bone include fibrous dysplasia, ossifying fibroma (osteofibrous dysplasia), and central low-grade osteosarcoma. Molecular classification of fibro-osseous lesions can be useful in differentiating these bone lesions. For example, fibrous dysplasia is marked by a mutation in the alpha subunit of the G protein of guanine nucleotide binding protein, alpha stimulating (*GNAS*) (Liang et al., 2011). Other immunohistochemical markers such as cyclin-dependent kinase 4 protein (CDK4) and murine double-minute type 2 protein (MDM2) help to differentiate benign fibro-osseous lesions from low-grade osteosarcomas (Dujardin et al., 2011). Identifying the genetic basis

of fibro-osseous lesions in the mouse provides the opportunity to compare these lesions on a molecular level and thereby to characterize novel model systems, which can be used to explore the human disease in greater depth.

This investigation aimed to identify the frequency and severity of fibro-osseous lesions of bone in 28 inbred and wild-derived mouse strains at various ages. Genome-wide scans were performed for female mice to identify the genetic variations associated with fibro-osseous lesions in this aging mouse population.

2. Materials and methods

2.1. Mice

The following 31 strains of inbred and wild-derived mice were used in a large-scale aging study (although only 28 strains survived to 20 months of age) (Sundberg et al., 2011; Yuan et al. 2009) and, as part of a detailed histopathological analysis, bones were examined for fibro-osseous lesions: 129S1/SvImJ, A/J, AKR/J, BALB/cByJ, BTBRT^{+}tf/J, BUB/BnJ, C3H/HeJ, C57BL/10J, C57BL/6J, C57BLKS/J, C57BR/cdJ, C57L/J, CAST/EiJ, CBA/J, DBA/2J, FVB/NJ, KK/HIJ, LP/J, MRL/MpJ, NOD.B10Sn-H2^{b}/J (NOD; a congenic strain with the NOD genetic background but with a histocompatibility locus from a diabetes-resistant strain), NON/ShiLtJ, NZO/HlLtJ, NZW/LacJ, P/J, PL/J, PWD/PhJ, RIIIS/J, SJL/J, SM/J, SWR/J, and WSB/J. Mice were part of a larger aging study by The Jackson Aging Center, which is described elsewhere (Sundberg et al., 2011). All mice were obtained from The Jackson Laboratory (Bar Harbor, ME) at 6 to 8 weeks of age and sacrificed in cohorts at 12 and 20 months of age (cross-sectional study) or were allowed to age and were collected when moribund (longitudinal study). Mice were euthanized by CO_2 asphyxiation using methods approved by the American Veterinary Medical Association (Leary et al., 2013) and complete necropsies were performed (Silva and Sundberg 2012).

The mouse rooms were maintained on a 12 h light/12 h dark cycle and at an ambient temperature of 21–23 °C. Mice of the same gender (4 per cage) were housed in duplex polycarbonate cages (31 × 31 × 214 cm) on pressurized individually ventilated mouse racks (Thoran Caging System; Hazleton, PA) with a high efficiency particulate air-filtered supply and exhaust. Mice were allowed ad libitum access to acidified water (pH 2.8–3.2) and fed pellets containing 6% fat (LabDiet 5K52, PMI Nutritional International, Bentwood, MO). Regular monitoring for viruses, bacteria, parasites, and microsporidium showed that the colonies were free of any infestation (http://jaxmice.jax.org/geneticheath/index.html). All protocols were reviewed and approved by The Jackson Laboratory Animal Care and Use Committee (Animal Use Summary #07005).

2.2. Tissue fixation and preparation

Complete necropsies were performed at the time of euthanasia (Silva and Sundberg 2012). Bones (i.e., calvaria, shoulder and elbow with associated long bones, hip and knee with associated long bones, ribs, and vertebrae from the thoracic, lumbar, and coccygeal regions) were collected, fixed in Fekete's acid-alcohol-formalin overnight, and stored in 70% ethanol until processing. Bones were decalcified overnight in Cal-Ex (Fisher, Pittsburgh, PA) and briefly rinsed in water before trimming. Once the bones were trimmed and placed into the

cassettes they were again rinsed in running water for a minimum of 4 h after which the tissues were processed routinely for histology, embedded in paraffin, cut into 6 μm sections, and stained with hematoxylin and eosin (H&E).

Additional serial sections were stained with Sirius Red and Mallory's trichrome stains for assessment of collagen deposition. Representative slides were subjected to immunohistochemistry for CD31 (Abcam cat# ab28364, Abcam, Cambridge, MA) as a marker of vascular endothelium (Ventana Medical Systems Discovery XT Automated Immunostainer, Oro Valley, AZ; http://tumor.informatics.jax.org/mtbwi/immunohistochemistry.jsp;jsessionid=747A7A0B4AE5B3AB58AF4CFDCDFE5496).

2.3. Histopathologic analysis

All tissue slides were reviewed by the same experienced, board certified veterinary pathologist (JPS) for histopathological analysis. Three strains (AKR/J, CAST/EiJ, and SJL/J)were not included in further analyses as they did not reach the age of 20 months (Sundberg et al., 2011). Fibro-osseous lesions were also evaluated by a board certified musculoskeletal pathologist (JMC) and compared to human archival clinical samples.

Prevalence of bone lesions was defined as the percentage of mice with diagnosed fibro-osseous lesions from the total number of mice per strain and gender (i.e., frequency). Lesions were also characterized by severity scores for each mouse (0 – normal; 1 – minimal; 2 – mild; 3 – moderate; 4 – severe). Average severity scores of all affected mice per strain and gender were calculated. Slides were reviewed and diagnoses were entered and coded by individual mouse using the Mouse Disease Information System (MoDIS) (Sundberg et al., 2009; Sundberg et al., 2008). Anatomical structures were defined using the Mouse Anatomy Ontology (MA) (Hayamizu et al., 2005) and disease diagnoses were entered using the Mouse Pathology ontology (MPATH) (Schofield et al., 2010a; Schofield et al., 2010b). Representative images of lesions in addition to those presented here are available on Pathbase (http://www.pathbase.net/) (Schofield et al., 2004a; Schofield et al., 2004b; Schofield et al. 2010b) and in the Mouse Tumor Biology Database (http://tumor.informatics.jax.org/) (Begley et al., 2014; Krupke et al., 2008).

2.4. Genome-wide association mapping

Genome-wide scans for frequency and severity of fibro-osseous lesions were performed using the expedited efficient mixed-model association (EMMAX) algorithm (Kang et al., 2010). Log-transformed strain frequencies of lesions in female mice were used as input data. The genome-wide scans were performed using four million (4 Mio. single nucleotide polymorphisms (SNP) by the NIEHS available for download at http://mouse.cs.ucla.edu/mousehapmap/full.html. Each SNP was evaluated individually and P-values were recorded as the strength of the genotype-phenotype associations.

2.5. Gene identification

Due to the possibility that the most significant SNPs are not the actual disease-causing variations but are inherited in co-segregation with true disease-causing variations, an arbitrary confidence interval of ±1 million base pairs (Mb) was applied around each

examined peak association and SNPs in this region were identified using The Jackson Laboratory's Mouse Genome Informatics tool (http://www.informatics.jax.org). SNPs were annotated using the Ensembl Genome Browser (Ensembl) Variant Effect Predictor tool (http://useast.ensembl.org/Homo_sapiens/UserData/UploadVariations). Ensembl's amino acid sequences of non-synonymous SNPs (CnSNPs) in the confidence interval surrounding the top three most significant hits were analyzed for predicted functional effects using the PolyPhen-2 (PPH2) predictor algorithm by the Sunyaev laboratory at Harvard (http://genetics.bwh.harvard.edu/pph2/) (Adzhubei et al. 2010).

2.6. Analysis of lesion data

Analyses of fibro-osseous lesions by strain and gender were performed using JMP 8 statistical analysis software (SAS institute; http://www.jmp.com/software/jmp8/).

2.7. Interacting partner identification

Interacting partners of candidate genes were searched on the Biogrid (Chatr-Aryamontri et al., 2015) and STRING (Szklarczyk et al., 2015) databases (last accessed 20.2.15).

3. Results

3.1. Fibro-osseous lesions in aging mice

Among all 28 analyzed strains, 370, 280, and 175 female and 362, 275, and 136 male mice were examined at 12 and 20 months of age, and the longitudinal study, respectively. Fibro-osseous lesions were found in 29 (8%), 80 (29%), and 20 (11%) female mice, but only in 0 (0%), 6 (1%), and 5 (4%) male mice in the respective age groups. In the two cross-sectional age groups specifically evaluated, the frequency of lesions increased with age. Lesions were essentially limited to females. Representative lesions for selected strains are illustrated in Figs. 1A–J and 2A–J.

Histologically, fibro-osseous lesions consisted of a cytologically uniform fibrovascular stroma interspersed with fine irregular trabeculae of woven bone. There was no evidence of cytologic atypia, mitotic activity, osteonecrosis, permeative growth patterns, cortical transgression, associated inflammation, or osteoblastic rimming. The presence of numerous intralesional blood vessels was confirmed using immunohistochemistry for an endothelial cell-specific marker (CD31, Fig. 2K and L).

3.2. Frequency and severity of fibro-osseous lesions among 28 strains

The frequency of mice with fibro-osseous lesions varied among strains (all per-strain data are available in Table 1). In female mice the case frequency ranged from 0% for 10 strains to 100% for KK/HlJ and NZW/LacJ mice (Table 1). We observed a strong gender dimorphism with regard to lesion incidence as few lesions were observed in male mice. Indeed, for 23 of the strains, no lesions were observed in males for any of the cohorts. Two anomalies to this pattern were noted from a statistical point of view, but these observations may be spurious do to small sample size. Specifically, for BUB/BnJ (Table 1) a 50% frequency rate was observed, but only 2 male mice were available for examination. Further, for BTBR T^{+} *Itpr3*^{tf}/J (2 of 6 evaluated), very few 20-month-old mice were available for

analysis and none of the 12-month-old male mice (13 and 14 mice per strain, respectively) had fibro-osseous lesions.

In an attempt to delineate severity, we compared the strains and scored the lesion using an index ranging from 0 (normal) to 4 (severe, Table 2). The highest average severity score was found for the 20-month-old KK/HlJ female mice (3.57). Frequency and severity were significantly correlated for both females (r^2=0.79; *P*-value <0.0001) and males (r^2=1; *P*-value <0.0001).

3.3. Correlation between fibro-osseous lesions and ovarian cysts

Previous reports suggested that fibro-osseous lesions are associated with hormonal imbalances related to ovarian cysts and endometrial cystic hyperplasia (Sass and Montali 1980). In this investigation, frequencies of fibro-osseous lesions in female mice were not significantly correlated with frequencies of ovarian follicular and bursal cysts (r = 0.18; P=0.36) or endometrial cystic hyperplasia (r=0.07; P=0.74).

The correlation was also not significant between strain-specific severities and ovarian (r = 0.11; P = 0.57) or endometrial (r = 0.03; P = 0.89) cyst formation frequency. Representative photomicrographs of ovarian and uterine lesions are available on Pathbase (http://www.pathbase.net) and the Mouse Tumor Biology Database (http://tumor.informatics.jax.org).

3.4. Correlation between fibro-osseous lesions and parathyroid gland abnormalities

Parathyroid Hormone (PTH), the hormone produced by the parathyroid gland, has profound effects on mineral homeostasis and bone physiology (Ito 2007; Silva et al. 2011). Abnormalities of bone structure may be associated with abnormalities in the parathyroid glands that result in altered PTH levels. The parathyroid glands are small organs in the laboratory mouse, but were collected and evaluated in most of the mice in this study. There were no histologic differences of the parathyroid gland between strains affected with fibro-osseous lesions and those totally unaffected (Fig. 1K–N). These results are consistent with other studies that found that the kidneys and parathyroids in affected mice were usually histologically normal (Frith and Ward 1988). No assays were done for PTH but serum chemistry was done for blood urea nitrogen and creatinine, which varied based on strain within normal parameters. Those strains with the most severe fibro-osseous lesions were within the middle of the strain distribution for these parameters (http://phenome.jax.org/).

3.5. Genome variants and their genes associated with susceptibility for fibro-osseous lesions

Genome-wide scans were performed using the EMMAX algorithm and a four million SNP panel by the NIEHS. Only female mice were evaluated due to the strong sexual dichotomy with phenotype presentation. Also, in this study only the strain distribution for frequency values was investigated because even after log-transformation severity values did not reach a normal distribution. Specifically, strain distribution of dichotomized frequency and logarithm of frequency was measured.

Twenty-month-old mice were measured in 28 strains as mice of the strains AKR/J, CAST/EiJ, and SJL/J did not reach this age (Sundberg et al., 2011). Frequency of fibro-osseous lesions was most strongly associated ($P < 10^{-6}$) with genome variations on chromosome (Chr) 8 at 90.6 and 90.8 Mb (rs33108071, rs33500669; $P = 5.0 \cdot 10^{-10}$, $1.3 \cdot 10^{-6}$), Chr 15 at 23.6 and 23.8 Mb (rs32087871, rs45770368; $P = 7.3 \cdot 10^{-7}$, $2.7 \cdot 10^{-6}$), and Chr 19 at 33.2, 33.4, and 33.6 Mb (rs311004232, rs30524929, rs30448815; $P = 2.8 \cdot 10^{-6}$, $2.8 \cdot 10^{-6}$, $2.8 \cdot 10^{-6}$) (Table 3). The top hit lies within an intron of the *Papd5* gene and a predicted enhancer (Regulatory feature: ENSMUSR00000668842) not yet known to be used in bone or connective tissue. Within a ±1 Mb region surrounding these top three hits, thirty-six genes contained coding region SNPs (CnSNPs), which were analyzed for potential functional importance using PPH2. Three genes on Chr 8 (*Rpgrip1l*, *Chd9*, and *Rbl2*) contained CnSNPs which are predicted to change the functions of the gene products (Table 4). The CnSNP of Rpgripl1l (RPGR-Interacting Protein 1-Like Protein) showed the highest probability for a functional change of its protein (PPH2 Prob=1) and was located 468 kb upstream of the significant SNP identified by the genome-wide scan. Twelve genes on Chr 19 (*Tcirg1*, *Mrpl21*, *LRP5*, *Ptprcap*, *Adrbki1*, *Nudt8*, *Ndufv1*, *Aldh3b1*, *BC021614*, *Ndufs8*, *Ighmbp2*, and *SSH3*) contained CnSNPs predicted to alter the function of their gene products (Table 4). CnSNPs in *Nudt8* (Nucleoside Diphosphate Linked Moiety X-Type Motif 8) and *Ssh3* (Slingshot Homolog 3) had a high probability of damaging the protein (PPH2 Prob=1), while a CnSNP in *Lrp5* (Low Density Lipoprotein Receptor-Related Protein 5) was the closest CnSNP on Chr 19 predicted to have significant effects on gene product function (PPH2 Prob = 0.997, distance from significant SNP = 264 kb) (Table 4).

4. Discussion

It is usual to associate similar or identical lesions with common metabolic or pathophysiological processes; the concept of phenotypic modularity. In the case of fibro-osseous lesions, previous reports followed this approach by suggesting that fibro-osseous lesions in a hybrid line of mice (B6C3F1) or limited number of inbred strains were hormone, and in particular estrogen, related (Highman et al., 1981; Sass and Montali 1980; Silberberg and Silberberg 1970; Sokoloff and Zipkin 1967). This implication was based on those lesions being diagnosed almost exclusively in females — particularly in females with ovarian cysts and endometrial cystic hyperplasia. In the study reported here, where 28 strains were studied systematically, there was no statistically significant correlation of ovarian cysts and endometrial cystic hyperplasia with fibro-osseous lesions. This suggests that the pathogenesis of fibro-osseous lesions in mice is due to other causes. Some strains, such as C3H/HeJ, one of the parental strains used to create the F1 hybrids B6C3F1 in previous studies, have a short reproductive cycle in production colonies due to poor fecundity (Flurky et al., 2009; Green and Witham 1997) associated with a high frequency of ovarian cysts and tubulostromal ovarian adenomas (Husler et al., 1998). The discrepancy between those previous observations and the study presented here is a good example how single inbred strain or F1 hybrid research cannot reproduce all facets of diseases with multiple etiologies.

Most previous reports of fibro-osseous lesions in mice involve the B6C3F1 hybrid stock (Gervais and Attia 2005; Sass and Montali 1980) in which lesions can be observed in mice

as young as 4.5 months of age. The sexual dichotomy is striking with 100% of females developing fibro-osseous lesions compared to only 1% of males by 16 months of age (Albassam et al., 1991; Sass and Montali 1980) This hybrid strain is made using a C57BL/6J female crossed with a C3H/HeJ male. Most reports describe hybrid stocks because these were commonly used in the large studies conducted by the National Center for Toxicological Research (NCTR) and the Carcinogenesis Testing Program of the National Cancer Institute (NCI) (Frith and Ward 1988). In our study, we focused only on inbred strains. As shown in Table 1, C57BL/6J and C3H/HeJ females had relatively low frequency of disease while 20% of males were affected in the very old C3H/HeJ longitudinal group only. While limited numbers of mice were available, this result suggests that there are environmental as well as genetic influences in the propensity to develop fibro-osseous lesions.

The most severely affected inbred strain in the study reported here (i.e., KK/HlJ) also develops systemic ectopic mineralization suggestive of a pseudoxanthoma elasticum-like (PXE-like) disease (Berndt et al., 2013; Berndt et al., 2014; Li et al., 2012). Fibro-osseous lesions suggest abnormalities in bone formation, which could be another aspect of the PXE-like disease. PXE is thought to be at least partially due to polymorphisms in the gene ATP-binding cassette, sub-family C (CFTR/MRP), member 6 (*Abcc6*). Among the 28 strains studied in the genome-wide investigations in this study, there were 4 non-synonymous SNPs in *Abcc6* (rs53235089: P = 0.02; rs53252134: P = 0.006; rs53254144: P=0.02; rs53257951: P=0.003) that were associated with frequency of fibro-osseous lesions. Therefore, *Abcc6* could be a link between the skin in PXE and bone lesions or could function as a modifier gene. Furthermore, 129S1/SvImJ, C3H/HeJ, and DBA/2J strains all have the same allelic mutation in *Abcc6* (Berndt et al., 2013) and all develop fibro-osseous lesions, albeit with different frequencies and severities. These strains also have PXE-like disease that varied in severity from most severe in KK/HlJ, intermediate in 129S1/SvImJ, to mild in C3H/HeJ and DBA/2J (Berndt et al., 2013). However, the other 18 strains that develop fibro-osseous lesions do not have this particular polymorphism which suggests that although *Abcc6* may be a modifier gene, it is unlikely to be the primary cause in this disease process.

Based on histopathological features, fibro-osseous disease in mice has some similarity to human Gorham-Stout Syndrome or Gorham's massive osteolysis/angiomatosis (Möller et al., 1999; van der Linden-van der Zwaag and Onvlee, 2006). This rare human disease is usually discovered during radiographic evaluation of pathologic fracture. Osteolysis is associated with fibrovascular stroma replacing normal bone marrow, as is the case with fibro-osseous disease in laboratory mice. In addition, CD31 immunohistochemistry disclosed an increased vascular density within the fibro-osseous lesions in mice. Fibro-osseous disease in mice was considered to be a relatively rare disease of aging until this strain survey was conducted. Routine histological evaluation of multiple bones revealed lesions, often initially in the calvaria, but scattered in many bones, suggesting that if bones are systematically evaluated in mice and humans, subtle lesions will be found revealing that this may be a common and overlooked disease in both species.

On chromosome 8 the most highly associated SNP lies within a predicted enhancer in intron 2 of *Papd5*. While this enhancer has not been shown to be active in bone or connective

tissue, the gene is known to regulate *miR21* which is involved in stem cell to osteoblast differentiation. Further investigation would be required to establish if this SNP or the surrounding enhancer altered the control of *Papd5* in fibro-osseous disease (Boele et al. 2014; Meng et al. 2015). Three further genes on Chr 8 (*Rpgrip1l*, *Chd9*, and *Rbl2*) contain CnSNPs which are predicted to change the functions of the gene products (Table 4). The CnSNP of *Rpgripl*1l (RPGR-Interacting Protein 1-Like Protein) showed the highest probability for a functional change of its protein (PPH2 Prob = 1) and was located 468 kb upstream of the significant SNP identified by the genome-wide scan. The protein coded for by Rpgrip1-like (*Rpgrip1l*) is located at the basal body of cilia. Null mutations in this gene in mice (*Rpgrip1l*^{tm1Urt}, *Rpgrip1l*$^{tm1a(EUCOMM)Wtsi}$) result in numerous developmental defects including abnormal bone development (Vierkotten et al., 2007), and it is one of the genes involved in the human ciliopathy, Joubert Syndrome (Arts et al., 2007; Delous et al., 2007). Chromodomain helicase DNA binding protein 9 (*Chd9*) is involved in chromatin remodeling and mesenchymal stem cell differentiation (Shur and Benayahu 2005). It has been shown to interact directly with *Esr1*, the estrogen receptor (Surapureddi et al., 2006), and is involved with osteogenic precursor differentiation (Benayahu et al., 2007; Shur et al., 2006). The known biology is certainly relevant to the phenotypes examined here but no phenotypes related to bone have been reported for the only allele to have been investigated, *Chd9*$^{tm1a(EUCOMM)Wtsi}$, although elevated alkaline phosphatase is seen in homozygous female mice (data from http://www.mousephenotype.org/, last viewed 1.11.15). No human variants have been linked to bone-related disease to date.

Retinoblastoma-like 2 (*Rbl2* ^{tm1Mru}) null mice have neurological developmental defects, which, in BALB/c mice, result in embryonic death (LeCouter et al., 1998). No skeletal evaluations were reported in these mice, however. Mice have not been created which carry other alleles (MGI). Twelve genes on Chr 19 (*Tcirg1*, *Mrpl21*, *Lrp5*, *Ptprcap*, *Adrbki1*, *Nudt8*, *Ndufv1*, *Aldh3b1*, *BC021614*, *Ndufs8*, *Ighmbp2*, and *Ssh3*) contained CnSNPs predicted to alter the function of their gene products (Table 4). Mice carrying homozygous mutant alleles of the T cell, immune regulator 1, ATPase, H+ transporting, lysosomal V0 protein A3 gene (*Tcirg1*) had severe osteopetrosis with increased bone density due to failure of secondary bone resorption. In addition, these mice lacked teeth and died around 30–40 days of age. (Li et al., 1999) *Tcirg1* interacts directly with *Abcc2* (Havugimana et al., 2012)which is another member of the ATP-binding cassette (ABC) transporter family of which *Abcc6* has been discussed above. *Abcc2* has itself been implicated in the pathobiology of PXE (Hendig et al., 2008). Human variants of *TCIRG1* have been strongly implicated in causing osseous disease and a wide spectrum of mutations in this gene is responsible form alignant infantile osteopetrosis (Sobacchi et al., 2001; Susani et al., 2004).

Mice with homozygous mutations in the low density lipoprotein receptor-related protein 5 gene (*Lrp5*) have various degrees of bone loss, decreased osteoblast proliferation, and a variety of other medical conditions related to organ systems other than the skeletal system, all of which depend on allelic combination and strain background, suggesting that this gene may have an important role as a genetic modifier of bone biology (Cui et al., 2011). While loss of LRP5 results in decreased bone mass because of decreased bone formation, LRP5 does not seem to be essential for the stimulatory effects of PTH on cancellous and cortical

bone formation (Iwaniec et al., 2007). It is, however, heavily implicated in bone physiology through human studies. It is the gene responsible for osteoporosis-pseudoglioma syndrome (Narumi et al., 2010), autosomal dominant osteopetrosis type I (VanWesenbeeck et al., 2003), and autosomal dominant endosteal hyperostosis (VanWesenbeeck et al., 2003). Variants in LRP5 have also been associated with osteoporosis in post-menopausal women (Sassi et al., 2014).

X-ray repair complementing defective repair in Chinese hamster cells 5 (*Xrcc5*) null mice is defective in DNA double-strand break repair and show impaired growth and severe combined immunodeficiency due to defective assembly of TCRs and immunoglobulins. Mutants die early with osteopenia, atrophic skin and hepatic abnormalities (Nussenzweig et al., 1996).

Mice null for protein tyrosine phosphatase, receptor type, C polypeptide-associated protein (*Ptprcap*) have impaired T and B cell responses to antigen receptor stimulation with no apparent bone abnormalities (Ding et al., 1999; Matsuda et al., 1998).

Targeted mutant mice for immunoglobulin mu binding protein 2 (*Ighmbp2*) die early, develop progressive limb muscle atrophy, decreased grip strength, severe motor neuron and axonal degeneration, dilated cardiomyopathy, myocardial fiber necrosis, increased heart rate variability, systolic dysfunction and respiratory failure, but without any reported bone phenotype (Cook et al., 1995; Krieger et al., 2013). Mutations in this gene cause Charcot-Marie-Tooth type 2S disease in humans but show no bone or connective tissue phenotypes apart from scoliosis (Cottenie et al., 2014).

Carnitine palmitoyltransferase 1a, liver (*Cpt1a*) homozygous null mice are embryonic lethals, while heterozygous null mice have decreased serum glucose and increased serum free fatty acid levels after fasting, but no recorded bone disease (Nyman et al., 2005). Similarly, in humans with PT deficiency, hepatic, type IA, there are no bone-related diseases (Gobin et al., 2002).

Dnajc19 (DnaJ (Hsp40) homolog, subfamily C, member 19) is responsible for 3-methylglutaconic aciduria, type V disease which shows no bone phenotypes (Davey et al., 2006). The only reported mouse mutant has broad effects on body growth, reduced hemoglobin levels, hypernatremia, hyperglycemia, and other metabolic disturbance (MGI: 4435205).

No live mice are currently available from ES cells containing various constructs of the mitochondrial ribosomal protein L21 (*Mrpl21*), nudix (nucleoside diphosphate linked moiety X)-type motif (*Nudt8*), PAP associated domain containing 5 (*Papd5*), cadherin 18 (*Cdh18*), CTD nuclear envelope phosphatase 1 regulatory subunit 1 (synonym *Tmem188*), aldehyde dehydrogenase 3 family, member B1 (*Aldh3b1*), cDNA sequence BC021614 (*BC021614*), or NADH dehydrogenase (ubiquinone) Fe–S protein 8 (*Ndufs8*) (MGI 3 Dec. 2015). *Adrbki1* and *Ndufy1* had no genes listed on MGI. Predicted gene 7729 (*Gm7729*) was listed as a pseudogene.

CnSNPs in *Nudt8* (Nucleoside Diphosphate Linked Moiety X-Type Motif 8) and *Ssh3* (Slingshot Homolog 3) had a high probability of damaging the protein (PPH2 Prob=1), while a CnSNP in *LRP5* (Low Density Lipoprotein Receptor-Related Protein 5) was the closest CnSNP on Chr 19 predicted to have significant effects on gene product function (PPH2 Prob = 0.997, Distance from significant SNP = 264 kb) (Table 4). All three of these genes are expressed in the osteoblast (PMID: 24945404) and additionally, *Ssh3* exhibits robust expression in the osteoclast (www.biogps.org).

These results indicate that fibro-osseous lesions are surprisingly common in many inbred strains of laboratory mice as they age. While this presents little problem in most studies that utilize young animals, it may complicate aging studies, particularly those focused on bone. The relatively large number of candidate genes identified in the GWAS analyses suggests that this may be an extremely complex polygenic disease. Variations in frequency from other published aging studies, using the same inbred or hybrid mice maintained at different facilities, further suggest that environment also plays a role in frequency of fibro-osseous disease within a particular strain. The relationship between this disease, in particular its severity, with pseudoxanthoma elasticum and the genes associated with it in humans and mouse models beyond *Abcc6* (Li and Uitto 2013) will require further investigation.

Acknowledgments

The authors thank Jesse Hammer for his assistance in preparing figures and tables.

Grants: This work was supported by grants from the Ellison Medical Foundation and the National Institutes of Health (AG025707, for the Jackson Aging Center and CA089713, for the Mouse Tumor Biology Database) and a fellowship by the Parker B. Francis foundation (to AB). The Jackson Laboratory Shared Scientific Services were supported in part by a Basic Cancer Center Core Grant from the National Cancer Institute (CA034196, to The Jackson Laboratory). PNS was supported by travel funds from Robinson College Cambridge.

Abbreviations

AB	Annerose Berndt
Abcc6	mouse ATP-binding cassette, sub-family C (CFTR/MRP), member 6 gene
CnSNPs	nonconsensus single nucleotide polymorphisms
CDK4	human cyclin-dependent kinase 4 protein
Ephb4	mouse ephrin receptor B4 gene
FGF23	human fibroblast growth factor 23 gene
Gigyf1	mouse GRB10 interacting GYF protein 1 gene
GNAS	human guanine nucleotide binding protein, alpha stimulating activity gene
IMPC	International Mouse Phenotyping Project
JMC	Justin M. Cates
JPS	John P. Sundberg
Mb	megabase

MDM2	murine double-minute type 2 protein
MoDIS	Mouse Disease Information System
MPD	Mouse Phenome Database
Pilra	mouse paired immunoglobin-like type 2 receptor alpha gene
PPH2	PolyPhen-2
PXE	pseudoxanthoma elasticum
SNPs	single nucleotide polymorphisms
Zkscan1	mouse zinc finger with KRAB and SCAN domains 1 gene

References

Adzhubei IA, et al. A method and server for predicting damaging missense mutations. Nat Methods. 2010; 7:248–249. [PubMed: 20354512]

Albassam MA, et al. Spontaneous fibro-osseous proliferative lesions in the sternums and femurs of B6C3F1 mice. Vet Pathol. 1991; 28:381–388. [PubMed: 1750163]

Arts HH, et al. Mutations in the gene encoding the basal body protein RPGRIP1L, a nephrocystin-4 interactor, cause Joubert syndrome. Nat Genet. 2007; 39:882–888. [PubMed: 17558407]

Begley DA, et al. Identifying mouse models for skin cancer using the Mouse Tumor Biology Database. Exp Dermatol. 2014; 23:761–763. [PubMed: 25040013]

Benayahu D, et al. Insights on the functional role of chromatin remodelers in osteogenic cells. Crit Rev Eukaryot Gene Expr. 2007; 17:103–113. [PubMed: 17725483]

Berndt A, et al. A single nucleotide polymorphism in the *Abcc6* gene associates with connective tissue mineralization in mice similar to targeted models for pseudoxanthoma elasticum. J Invest Dermatol. 2013; 133:833–836. [PubMed: 23014343]

Berndt A, et al. Phenotypic characterization of the KK/HlJ inbred mouse strain. Vet Pathol. 2014; 51:846–857. [PubMed: 24009271]

Boele J, et al. PAPD5-mediated 3′ adenylation and subsequent degradation of miR-21 is disrupted in proliferative disease. Proc Nat Acad Sci USA. 2014; 111:11467–11472. [PubMed: 25049417]

Chatr-Aryamontri A, et al. The BioGRID interaction database: 2015 update. Nucleic Acids Res. 2015; 43:D470–478. [PubMed: 25428363]

Cook SA, et al. Neuromuscular degeneration (nmd): a mutation on mouse chromosome 19 that causes motor neuron degeneration. Mamm Genome. 1995; 6:187–191. [PubMed: 7749225]

Cottenie E, et al. Truncating and missense mutations in IGHMBP2 cause Charcot-Marie Tooth disease type 2. Am J Hum Genet. 2014; 95:590–601. [PubMed: 25439726]

Cui Y, et al. Lrp5 functions in bone to regulate bone mass. Nat Med. 2011; 17:684–691. [PubMed: 21602802]

Davey KM, et al. Mutation of DNAJC19, a human homologue of yeast inner mitochondrial co-chaperones, causes DCMA syndrome, a novel autosomal recessive Barth syndrome-like condition. J Med Genet. 2006; 43:385–393. [PubMed: 16055927]

Delous M, et al. The ciliary gene RPGRIP1L is mutated in cerebello-oculo-renal syndrome (Joubert syndrome type B) and Meckel syndrome. Nature Genet. 2007; 39:875–881. [PubMed: 17558409]

Ding I, et al. Biochemical and functional analysis of mice deficient in expression of the CD45-associated phosphoprotein LPAP. Eur J Immunol. 1999; 29:3956–3961. [PubMed: 10602004]

Dodd DC, Port CD. Hyperostosis of the marrow cavity caused by misoprostol in CD-1 strain mice. Vet Pathol. 1987; 24:545–548. [PubMed: 3137716]

Dujardin F, et al. MDM2 and CDK4 immunohistochemistry is a valuable tool in the differential diagnosis of low-grade osteosarcomas and other primary fibro-osseous lesions of the bone. Mod Pathol. 2011; 24:624–637. [PubMed: 21336260]

Elefteriou F, Yang X. Genetic mouse models for bone studies—strengths and limitation. Bone. 2011; 49:1242–1254. [PubMed: 21907838]

Flurky, K., et al. The Jackson Laboratory Handbook on Genetically Standardized Mice. The Jackson Laboratory; Bar Harbor, ME: 2009.

Frith, CH.; Ward, JM. Color Atlas of Neoplastic and non-Neoplastic Lesions in Aging Mice. Elsevier; Amsterdam: 1988.

Gervais F, Attia MA. Fibro-osseous proliferation in the sternums and femurs of female B6C3F1, C57black and CD-1 mice: a comparative study. Dtsch Tierarztl Wochenschr. 2005; 112:323–326. [PubMed: 16240910]

Gobin S, et al. Organization of the human liver carnitine palmitoyltransferase 1 gene (CPT1A) and identification of novel mutations in hypoketotic hypoglycaemia. Hum Genet. 2002; 111:179–189. [PubMed: 12189492]

Green, MC.; Witham, BA. Handbook of Genetically Standardized Jax Mice. The Jackson Laboratory; Bar Harbor, ME: 1997.

Havugimana PC, et al. A census of human soluble protein complexes. Cell. 2012; 150:1068–1081. [PubMed: 22939629]

Hayamizu TF, et al. The adult mouse anatomical dictionary: a tool for annotating and integrating data. Genome Biol. 2005; 6:R29. [PubMed: 15774030]

Hendig D, et al. Gene expression profiling of ABC transporters in dermal fibroblasts of pseudoxanthoma elasticum patients identifies new candidates involved in PXE pathogenesis. Lab Investig. 2008; 88:1303–1315. [PubMed: 18936737]

Highman B, et al. Osseous changes and osteosacomas in mice continuously fed diets containing diethylstilbestrol or 17 beta-estradiol. J Natl Cancer Inst. 1981; 67:653–662. [PubMed: 6944535]

Husler MR, et al. Neoplastic and hyperplastic lesions in aging C3H/HeJ mice. J Exp Anim Sci. 1998; 38:165–180.

Ito M. Parathyroid and bone. Effect of parathyroid hormone on bone quality. Clin Calcium. 2007; 17:1858–1864. [PubMed: 18057661]

Iwaniec UT, et al. PTH stimulates bone formation in mice deficient in Lrp5. J Bone Miner Res. 2007; 22:394–402. [PubMed: 17147489]

Kang HM, et al. Variance component model to account for sample structure in genome-wide association studies. Nat Genet. 2010; 42:348–354. [PubMed: 20208533]

Kavirayani AM, Foreman O. Retrospective study of spontaneous osteosarcomas in the nonobese diabetic strain and nonobese diabetic-derived substrains of mice. Vet Pathol. 2010; 47:482–487. [PubMed: 20348488]

Kavirayani AM, et al. Pathology of bone tumors in mice: retrospective study and review of the literature. Vet Pathol. 2012; 49:182–205. [PubMed: 21343597]

Krieger F, et al. Fast motor axon loss in SMARD1 does not correspond to morphological and functional alterations of the NMJ. Neurobiol Dis. 2013; 54:169–182. [PubMed: 23295857]

Krupke D, et al. The mouse tumor biology database. Nat Rev Cancer. 2008; 8:459–465. [PubMed: 18432250]

Leary, S., et al. AVMA Guidelines for the Euthanasia of Animals: 2013 Edition. American Veterinary Medical Association; Schaumburg, IL: 2013. p. 1-102.

LeCouter JE, et al. Strain-dependent embryonic lethality in mice lacking the retinoblastoma-related p130 gene. Development. 1998; 125:4669–4679. [PubMed: 9806916]

Li Q, Uitto J. Mineralization/anti-mineralization networks in the skin and vascular connective tissues. Am J Pathol. 2013; 183:10–18. [PubMed: 23665350]

Li YP, et al. Atp6i-deficient mice exhibit severe osteopetrosis due to loss of osteoclast-mediated extracellular acidification. Nat Genet. 1999; 23:447–451. [PubMed: 10581033]

Li Q, et al. A novel animal model for pseudoxanthoma elasticum — the KK/H1J mouse. Am J Pathol. 2012; 181:1190–1196. [PubMed: 22846719]

Liang Q, et al. Quantitative analysis of activating alpha subunit of the G protein (Gsalpha) mutation by pyrosequencing in fibrous dysplasia and other bone lesions. J Mol Diagn. 2011; 13:137–142. [PubMed: 21354047]

Matsuda A, et al. Disruption of lymphocyte function and signaling in CD45-associated protein-null mice. J Exp Med. 1998; 187:1863–1870. [PubMed: 9607926]

Meng YB, et al. microRNA-21 promotes osteogenic differentiation of mesenchymal stem cells by the PI3K/β-catenin pathway. J Orthop Res. 2015; 33:957–964. [PubMed: 25728838]

Möller G, et al. The Gorham-Stout syndrome (Gorham's massive osteolysis). A report of six cases with histopathological findings. J Bone Joint Surg Br. 1999; 81:501–506. [PubMed: 10872375]

Narumi S, et al. Various types of LRP5 mutations in four patients with osteoporosis-pseudoglioma syndrome: identification of a 7.2-kb microdeletion using oligonucleotide tiling microarray. Am J Med Genet. 2010; 152A:133–140. [PubMed: 20034086]

Nussenzweig A, et al. Requirement for Ku80 in growth and immunoglobulin V(D)J recombination. Nature. 1996; 382:551–555. [PubMed: 8700231]

Nyman LR, et al. Homozygous carnitine palmitoyltransferase 1a (liver isoform) deficiency is lethal in the mouse. Mol Genet Metab. 2005; 86:179–187. [PubMed: 16169268]

Sass B, Montali RJ. Spontaneous fibro-osseous lesions in aging female mice. Lab Anim Sci. 1980; 30:907–909. [PubMed: 7431877]

Sass B, et al. Differences in tumor incidence in two substrains of Claude BALB/c (BALB/cfCd) mice, emphasizing renal, mammary, pancreatic, and synovial tumors. Lab Anim Sci. 1976; 26:736–741. [PubMed: 185454]

Sassi R, et al. Association of LRP5 genotypes with osteoporosis in Tunisian post-menopausal women. BMC Musculoskelet Disord. 2014; 15:144. [PubMed: 24885293]

Schofield PN, et al. Pathbase: a new reference resource and database for laboratory mouse pathology. Radiat Prot Dosim. 2004a; 112:525–528.

Schofield PN, et al. Pathbase: a database of mutant mouse pathology. Nucleic Acids Res. 2004b; 32:D512–515. [PubMed: 14681470]

Schofield PN, et al. Phenotype ontologies for mouse and man: bridging the semantic gap. Dis Model Mech. 2010a; 3:281–289. [PubMed: 20427557]

Schofield PN, et al. Pathbase and the MPATH ontology: community resources for mouse histopathology. Vet Pathol. 2010b; 47:1016–1020. [PubMed: 20587689]

Shur I, Benayahu D. Characterization and functional analysis of CReMM, a novel chromodomain helicase DNA-binding protein. J Mol Biol. 2005; 352:646–655. [PubMed: 16095617]

Shur I, et al. Dynamic interactions of chromatin-related mesenchymal modulator, a chromodomain helicase-DNA-binding protein, with promoters in osteoprogenitors. Stem Cells. 2006; 24:1288–1293. [PubMed: 16705189]

Silberberg M, Silberberg R. Age-linked modification of the effect of estrogen on joints and cortical bone of female mice. Gerontologia. 1970; 16:201–211. [PubMed: 5482369]

Silva, KA.; Sundberg, JP. Necropsy Methods. In: Hedrich, HJ., editor. The Laboratory Mouse. Academic Press; London: 2012. p. 779-806.

Silva BC, et al. Catabolic and anabolic actions of parathyroid hormone on the skeleton. J Endocrinol Investig. 2011; 34:801–810. [PubMed: 21946081]

Sobacchi C, et al. The mutational spectrum of human malignant autosomal recessive osteopetrosis. Hum Mol Genet. 2001 Aug 15; 10(17):1767–1773. [PubMed: 11532986]

Sokoloff L, Habermann RT. Idiopathic necrosis of bone in small laboratory animals. AMA Arch Pathol. 1958; 65:322–330. [PubMed: 13507818]

Sokoloff L, Zipkin I. Odontogenic hamartomas in an inbred strain of mouse (STR-1N). Proc Soc Exp Biol Med. 1967; 124:147–149. [PubMed: 6017757]

Sundberg JP, et al. Integrating mouse anatomy and pathology ontologies into a diagnostic/phenotyping database: tools for record keeping and teaching. Mamm Genome. 2008; 19:413–419. [PubMed: 18797968]

Sundberg BA, et al. A data capture tool for mouse pathology phenotyping. Vet Pathol. 2009; 46:1230–1240. [PubMed: 19605915]

Sundberg JP, et al. The mouse as a model for understanding chronic diseases of aging: the histopathologic basis of aging in inbred mice. Pathobiol Aging Age-related Dis. 2011; 1:7179. DOI: http://dx.doi.org/10.3402/pba.v1i0.7179.

Surapureddi S, et al. PRIC320, a transcription coactivator, isolated from peroxisome proliferator-binding protein complex. Biochem Biophys Res Commun. 2006; 343:535–543. [PubMed: 16554032]

Susani L, et al. TCIRG1-dependent recessive osteopetrosis: mutation analysis, functional identification of the splicing defects, and in vitro rescue by U1 snRNA. Hum Mutat. 2004; 24:225–235. [PubMed: 15300850]

Szklarczyk D, et al. STRING v10: protein-protein interaction networks, integrated over the tree of life. Nucleic Acids Res. 2015; 43:D447–452. [PubMed: 25352553]

van der Linden-van der Zwaag H, Onvlee GJ. Massive osteolysis (Gorham's disease) affecting the femur. Acta Orthop Belg. 2006; 72:261–268. [PubMed: 16889136]

VanWesenbeeck L, et al. Six novel missense mutations in the LDL receptor-related protein 5 (LRP5) gene in different conditions with an increased bone density. Am J Hum Genet. 2003; 72:763–771. [PubMed: 12579474]

Vierkotten J, et al. Ftm is a novel basal body protein of cilia involved in Shh signalling. Development. 2007; 134:2569–2577. [PubMed: 17553904]

Woodward, JC.; Montgomery, CA. Musculoskeletal system. In: Bernirschke, K., et al., editors. Pathology of Laboratory Animals. Springer; New York: 1978. p. 664-820.

Yuan R, et al. Aging in inbred strains of mice: study design and interim report on median lifespans and circulating IGF1 levels. Aging Cell. 2009; 8:277–287. [PubMed: 19627267]

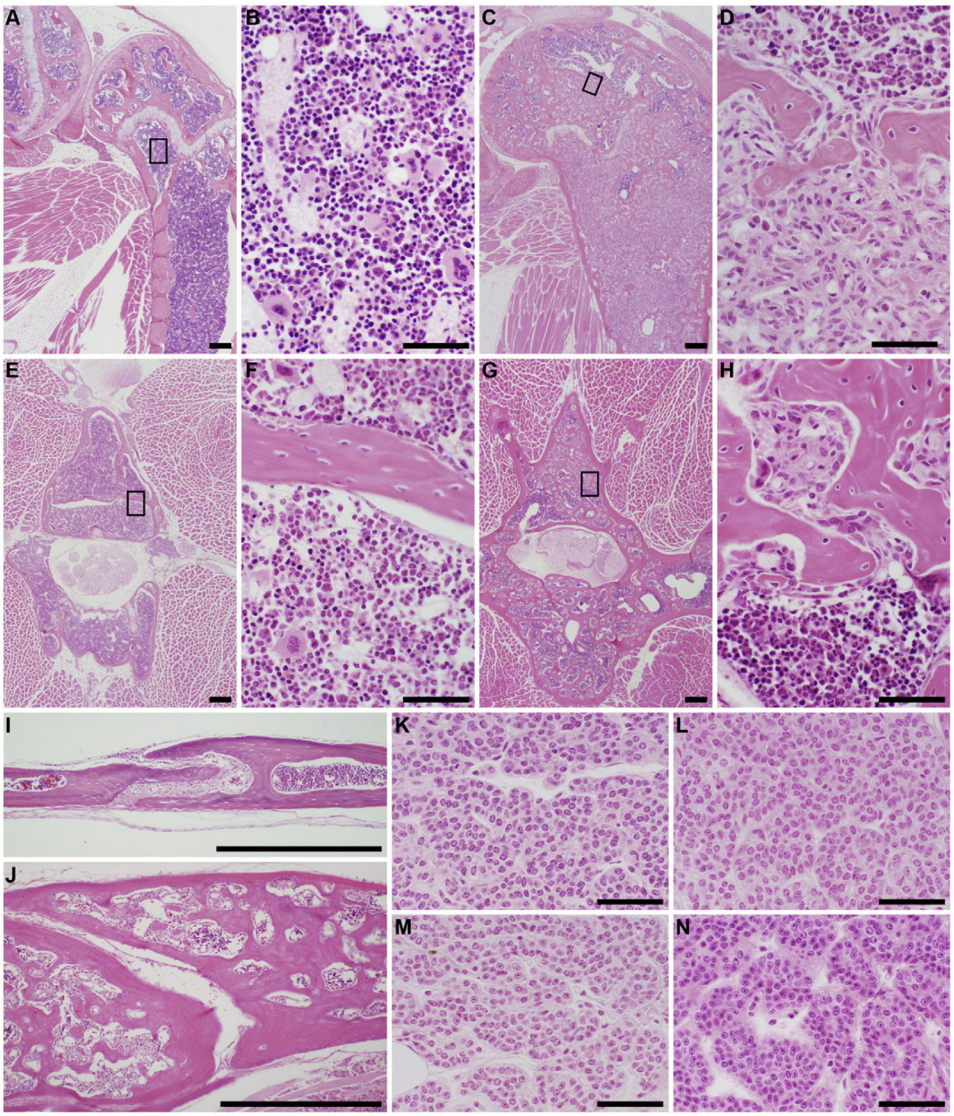

Fig. 1.

Femur (knee joint)with normal cortical bone and marrow cavity (blue, A, B, female LP/J, 372 days old) compared to diffuse fibro-osseous lesions (C, D, female KK/HlJ, 586 days old). Boxed areas in low magnification overview (A, C) are enlarged in the image to the right (B, D). Normal lumbar vertebral body (E, F, female DBA/2 J, 618 days old) compared to a moderate case of fibro-osseous lesion (G, H, female LP/J, 621 days old). Suture in the calvaria of normal bone (I, female SWR/J, 395 day old) and thickened bone due to fibro-osseous lesions (J, female KK/HlJ, 418 days old). Parathyroid glands from KK/HlJ female mice with fibro-osseous lesions (K, 427 days old, L, 647 days old) are indistinguishable from those from C57BL/6J females with normal bones (M, 372 days old, N, 908 days old).

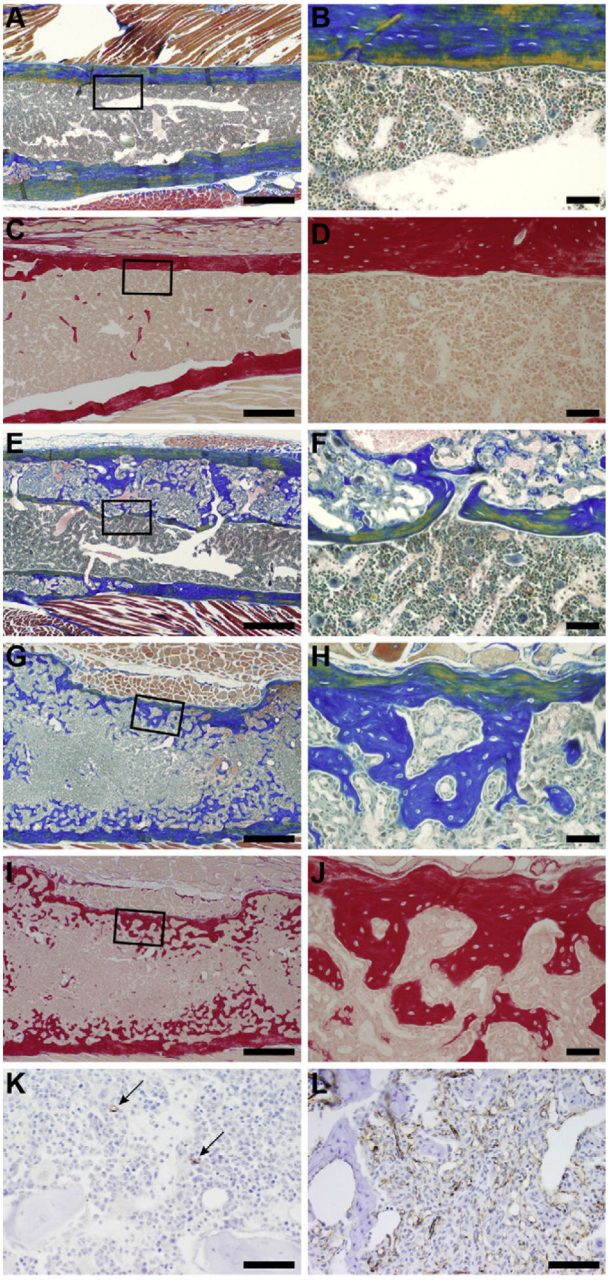

Fig. 2.

Femurs from an LP/J female (372 days, A–D, essentially normal bone and marrow), LP/J female (621 days, E, F, moderate, localized fibro-osseous lesions), and KK/HlJ female (586 days, G–J, severe diffuse fibro-osseous lesions) stained with Mallory's (A, B, E–H) and Sirius Red (C, D, I, J). Note the decreasing thickness of cortical bone and increase in medullary trabeculae as the disease progresses. Left column 4× (bar=200 μm), right column 25× (bar=50 μm). Immunohistochemistry localization of CD31 for endothelial cells reveals few capillaries in the normal bone marrow of a 372 day old LP/J female compared to

numerous vascular spaces in the 427 day old KK/HlJ female mouse with severe diffuse fibro-osseous lesions that completely efface the bone marrow cavity. 40×, Bar = 20 μm.

Table 1

Number of diagnoses, mice, and frequency of fibro-osseous lesions per strain in different age groups.

Sex	Strain	12-month-group			20-month-group			Longitudinal group		
		Diagn	Mice	Freq	Diagn	Mice	Freq	Diagn	Mice	Freq
Females	129S1SvImJ	2	15	13	12	13	92	1	1	100
	A/J	0	13	0	0	7	0	0	19	0
	BALB/cByJ	0	14	0	2	15	13	0	12	0
	BTBRT< + >tf/J	0	19	0	2	7	29	0	2	0
	BUB/BnJ	0	13	0	0	9	0	0	3	0
	C3H/HeJ	0	9	0	0	6	0	1	13	8
	C57BL/10J	0	14	0	5	12	42	0	4	0
	C57BL/6J	0	15	0	2	15	13	0	6	0
	C57BLKS/J	1	12	8	1	13	0	0	12	0
	C57BR/cdJ	0	14	0	3	11	0	1	5	20
	C57L/J	0	15	0	1	15	7	0	1	0
	CBA/J	0	15	0	3	13	27	0	8	0
	DBA/2J	1	12	8	2	7	29	1	5	20
	FVB/NJ	0	14	0	2	6	33	3	8	38
	KK/HlJ	14	15	93	7	7	100	4	4	100
	LP/J	2	15	13	10	13	69	0	2	0
	MRL/MpJ	3	15	20	1	7	14	2	26	8
	NOD	0	12	0	1	8	13	0	4	0
	NON/LtJ	0	13	0	0	13	0	0	9	0
	NZO/HlLtJ	1	12	8	2	6	33	0	0	NA
	NZW/LacJ	0	15	0	8	8	100	2	2	100
	P/J	0	0	NA	2	10	20	0	3	0
	PL/J	0	9	0	0	5	0	0	1	0
	PWD/PhJ	0	15	0	0	13	0	0	6	0
	RIIIS/J	0	14	0	4	14	29	1	8	12
	SM/J	0	15	0	0	11	0	0	2	0
	SWR/J	1	13	8	0	5	0	0	6	0

Sex	Strain	12-month-group			20-month-group			Longitudinal group		
		Diagn	Mice	Freq	Diagn	Mice	Freq	Diagn	Mice	Freq
	WSB/EiJ	4	13	31	10	11	91	2	3	67
Summary		29	370	8	80	280	29	20	175	11
Males	129S1/SvImJ	0	15	0	1	15	7	0	12	0
	A/J	0	13	0	0	9	0	0	10	0
	BALB/cByJ	0	14	0	0	9	0	0	4	0
	BTBRT< + >tf/J	0	13	0	2	6	33	0	4	0
	BUB/BnJ	0	10	0	1	2	50	0	0	NA
	C3H/HeJ	0	14	0	0	10	0	0	5	0
	C57BL/10J	0	14	0	0	14	0	0	7	0
	C57BL/6J	0	15	0	0	14	0	2	10	20
	C57BLKS/J	0	15	0	0	15	0	0	13	0
	C57BR/cdJ	0	16	0	0	15	0	1	3	33
	C57L/J	0	15	0	0	14	0	0	2	0
	CBA/J	0	14	0	0	11	0	0	7	0
	DBA/2J	0	11	0	0	6	0	0	7	0
	FVB/NJ	0	15	0	0	7	0	0	4	0
	KK/HlJ	0	12	0	1	7	14	1	3	33
	LP/J	0	15	0	0	14	0	0	8	0
	MRL/MpJ	0	15	0	0	10	0	0	6	0
	NOD	0	12	0	0	9	0	0	1	0
	NON/LtJ	0	15	0	0	12	0	0	2	0
	NZO/HlLtJ	0	5	0	0	5	0	0	2	0
	NZW/LacJ	0	14	0	1	10	10	0	3	0
	P/J	0	3	0	0	6	0	0	0	NA
	PL/J	0	17	0	0	2	0	0	1	0
	PWD/PhJ	0	12	0	0	10	0	0	6	0
	RIIIS/J	0	15	0	0	12	0	0	5	0
	SM/J	0	13	0	0	13	0	0	4	0
	SWR/J	0	7	0	0	7	0	0	5	0
	WSB/EiJ	0	13	0	0	11	0	1	2	50

Sex	Strain	12-month-group			20-month-group			Longitudinal group		
		Diagn	Mice	Freq	Diagn	Mice	Freq	Diagn	Mice	Freq
Summary		0	362	0	6	275	2	5	136	4

Diagn, diagnosis; Freq, frequency.

Table 2

Average severity of fibro-osseous lesions in female mice per strain in different age groups.

Sex	Strain	12 month	20 month	Longitudinal group
Female	129S1/SvImJ	1.5	1.75	3.0
	A/J	–	0.0	–
	BALB/cByJ	–	1.5	–
	BTBRT< + >tf/J	–	1.0	–
	BUB/BnJ	–	0.0	–
	C3H/HeJ	–	0.0	1.0
	C57BL/10J	–	1.0	–
	C57BL/6J	–	1.0	–
	C57BLKS/J	1.0	1.0	–
	C57BR/cdJ	–	1.0	2.0
	C57L/J	–	3.0	–
	CBA/J	–	2.33	–
	DBA/2 J	3.0	1.0	1.0
	FVB/NJ	–	1.5	1.33
	KK/HlJ	2.78	3.57	3.5
	LP/J	1.0	1.2	–
	MRL/MpJ	1.0	1.0	2.0
	NOD	–	1.0	–
	NON/LtJ	–	0.0	–
	NZO/HlLtJ	2.0	1.0	–
	NZW/LacJ	–	1.5	2.0
	P/J	–	1.5	–
	PL/J	–	0.0	–
	PWD/PhJ	–	0.0	–
	RIIIS/J	–	2.25	1.0
	SM/J	–	0.0	–
	SWR/J	2.0	0.0	–
	WSB/EiJ	1.5	2.5	1.0
Average		2.1	1.78	1.9
Male	129S1Sv/ImJ	–	1.0	–
	A/J	–	–	–
	BALB/cByJ	–	–	–
	BTBRT< + >tf/J	–	1.0	–
	BUB/BnJ	–	–	–
	C3H/HeJ	–	1.0	–
	C57BL/10J	–	–	–
	C57BL/6J	–	–	2.0
	C57BLKS/J	–	–	–
	C57BR/cdJ	–	–	1.0

Sex	Strain	12 month	20 month	Longitudinal group
	C57L/J	–	–	–
	CBA/J	–	–	–
	DBA/2J	–	–	–
	FVB/NJ	–	–	–
	KK/HlJ	–	1.0	1.0
	LP/J	–	–	–
	MRL/MpJ	–	–	–
	NOD	–	–	–
	NON/LtJ	–	–	–
	NZO/HlLtJ	–	–	–
	NZW/LacJ	–	1.0	–
	P/J	–	–	–
	PL/J	–	–	–
	PWD/PhJ	–	–	–
	RIIIS/J	–	–	–
	SM/J	–	–	–
	SWR/J	–	–	–
	WSB/EiJ	–	–	1.0
Average			1.0	1.4

Table 3

SNPs most significantly associated with dichotomized frequency of fibro-osseous lesions and logarithmic frequency of fibro-osseous lesions. The closest gene to the SNP is identified including distance to the gene if intergenic. *P*-values are for dichotomized frequency (dFreq) and logarithmic frequency (logFreq).

SNP ID	Chr	Position	Gene	Gene name	SNP relation to gene	Distance from gene	*P*-value (dFreq)	*P*-value (logFreq)
rs33108071	8	90751852	*Papd5*	PAP Associated Domain Containing 5	Intronic		5.01426e-10	1.39198e-07
rs32087871	15	23621293	*Cdh18*	Cadherin 18	Intergenic	217 kb	7.24642e-07	5.42675e-05
rs33500669	8	90618689	*Tmem188*	CTD nuclear envelope phosphatase 1 regulatory subunit 1	Intergenic	23.7 kb	1.33160e-06	3.54036e-05
rs45770368	15	23885266	*Cdh18*	Cadherin 18	Intergenic		2.71569e-06	
rs31004232	19	3319089	*Cpt1A*	Carnitine palmitoyltransferase 1A	Intergenic	4.2 kb	2.75266e-06	7.76579e-06
rs30524929	19	3344381	*Cpt1A*	Carnitine palmitoyltransferase 1A	Intronic		2.75266e-06	7.76579e-06
rs30448815	19	3366276	*Cpt1A*	Carnitine palmitoyltransferase 1A	Intronic		2.75266e-06	7.76579e-06
rs31534292	18	27559918	*Gm7729*	Heterogeneous nuclear ribonucleoprotein A1 pseudogene	Intergenic	197.2 kb	4.54441e-06	8.21717e-06
rs31536363	18	27581952	*Gm7729*	Heterogeneous nuclear ribonucleoprotein A1 pseudogene	Intergenic	175.1 kb	4.54441e-06	8.21717e-06
rs30524680	01	72409588	*Xrcc5*	X-ray repair complementing defective repair in Chinese Hamster Cells 5	Intronic		8.86502e-06	3.18017e-05
rs29893269	03	34176862	*Dnajc19*	DnaJ (Hsp40) Homolog, subfamily C, member 19	Intergenic	196.6 kb	9.92306e-06	

Table 4

CnSNPs with predicted functional change to the gene product located in the ±1 Mb region around the most significantly associated SNPs identified by genome-wide scan for dichotomized fibro-osseous lesion frequency.

rsNumber	Chr	Position	UniProt gene name	AA position	AA1	AA2	PPH2 prediction	PPH2 Prob	PPH2 FPR	PPH2 TPR	Significant SNP	Distance to significant SNP
rs13471558	19	3904246	*Tcirg1*	56	R	Q	Probably damaging	0.987	0.036	0.731	rs30448815	538 kb
rs37227651	19	3283148	*Mrpl21*	26	L	S	Possibly damaging	0.505	0.0966	0.883	rs31004232	36 kb
rs31109187	19	3652157	*Lrp5*	220	R	H	Possibly damaging	0.928	0.058	0.806	rs30448815	286 kb
rs36423656	19	4156330	*Ptprcap*	137	Q	H	Possibly damaging	0.827	0.0695	0.838	rs30448815	790 kb
rs36467241	19	4289356	*Adrbk1*	387	L	V	Probably damaging	0.998	0.0112	0.273	rs30448816	923 kb
rs36600575	19	4001698	*Nudt8*	90	L	P	Probably damaging	1	0.00026	0.00018	rs30448817	635 kb
rs36770449	19	4011407	*Ndufv1*	32	F	L	Possibly damaging	0.746	0.0783	0.853	rs30448818	645 kb
rs37082918	8	91220214	*Rpgrip1l*	1253	S	F	Probably damaging	1	0.00026	0.00018	rs33108071	468 kb
rs37186928	19	4156233	*Ptprcap*	105	P	R	Probably damaging	0.988	0.0353	0.727	rs30448817	790 kb
rs37257011	19	3923893	*Aldh3b1*	3	S	W	Probably damaging	0.987	0.036	0.731	rs30448818	558 kb
rs37545229	19	4057961	*Bco21614*	124	P	L	Probably damaging	0.972	0.0442	0.766	rs30448819	692 kb
rs37755589	19	3911585	*Ncufs8*	30	S	R	Possibly damaging	0.849	0.0674	0.834	rs30448820	545 kb
rs37994963	19	4008109	*Ndufv1*	367	I	M	Probably damaging	0.994	0.0289	0.689	rs30448821	642 kb
rs38037222	19	3265302	*Ighmbp2*	706	S	F	Possibly damaging	0.83	0.0692	0.837	rs31004232	54 kb
rs38435684	19	3630364	*Lrp5*	373	H	Q	Probably damaging	0.997	0.0167	0.409	rs30448819	264 kb
rs38770011	19	4001229	*Nudt8*	76	Q	H	Possibly damaging	0.803	0.0723	0.842	rs30448820	635 kb
rs38991759	19	4262555	*Ssh3*	583	K	N	Possibly damaging	0.52	0.096	0.882	rs30448821	896 kb
rs39828615	19	4264447	*Ssh3*	356	L	M	Probably damaging	1	0.00026	0.00018	rs30448822	898 kb
rs45831590	8	91034908	*Chd9*	2207	G	D	Probably damaging	0.999	0.00574	0.136	rs33108071	283 kb
rs45837294	8	91090167	*Rbl2*	428	T	S	Probably damaging	0.986	0.0368	0.736	rs33108072	338 kb
rs49308844	8	91051370	*Chd9*	2670	G	S	Probably damaging	0.999	0.00574	0.136	rs33108073	300 kb
rs6401135	19	3268715	*Ighmbp2*	454	A	P	Possibly damaging	0.92	0.0592	0.81	rs31004232	50 kb